Homodyne chopper for weak optical signal detection

Jerzy Siuzdak, Roman Nowak, Tomasz Czarnecki

Telecommunications Institute, Warsaw University of Technology, ul Nowowiejska 15/19, 00–665 Warszawa, Poland.

In the paper, a homodyne chopper for weak optical signal detection meant for monochromators is described. The software used is also shortly discussed. Some design problems are mentioned, including the selection of operating frequency, optimisation of noise, and the choice of diaphragm shape. The measurement errors are also analysed. It follows that monochromator errors and photodetector sensitivity errors play the main role.

1. Introduction

A monochromator is one of the most important instruments which measure optical signal spectrum. It is often used in modern measuring equipment such as optical spectrum analysers. In a frequently employed configuration (Czerny–Turner [1]), the optical spectrum is formed by a flat rotating reflective grating equipped with two spherical mirrors. A given wavelength is selected by a narrow slot followed by a photodetector. A low optical power as compared to the photodetector noise level is a common problem, especially for low power optical sources with broad linewidth. A solution to this problem is the amplitude modulation of the optical flux together with homodyne detection at the receiver.

In this paper, a chopper developed at the Institute of Telecommunications of the Warsaw University of Technology is described. This instrument may work with any monochromator. A short description of the chopper operating principle is given. Design problems and measurement errors are discussed as well. Due to unique design, namely simultaneous modulation of both the measured signal and the reference, the chopper is practically insensitive to the signal phase fluctuation and rotating speed variation.

2. Operating principle

A block scheme of the chopper is shown in Fig. 1. The operating principle is simple. The power of the measured optical signal is modulated by a rotating disc with openings. The same disc simultaneously modulates the power of the reference channel which consists of an optical transducer and a forming circuit (comparator). As shown in the next section, such a design makes the instrument insensitive to
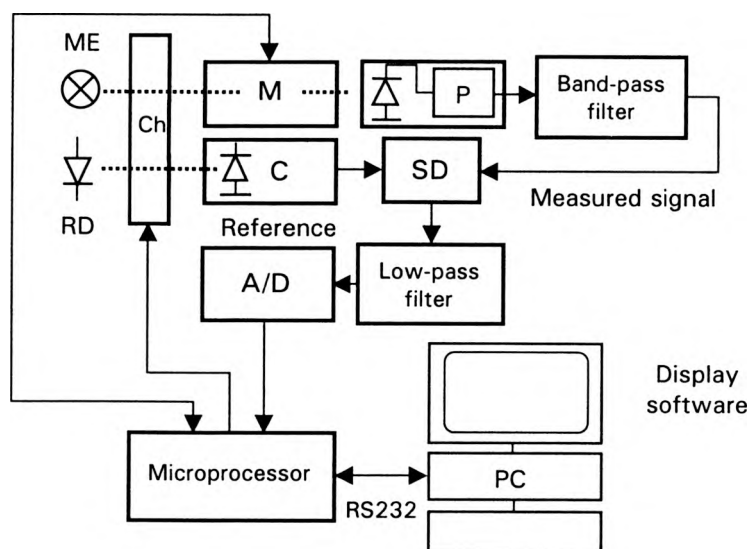
Fig. 1. Block scheme of the chopper: P — preamplifier, Ch — chopper, ME — measured element, RD — reference diode, M — monochromator, C — comparator, SD — synchronizing detector.

the rotating speed variation. The measured signal arrives at the input of the monochromator. The current position of the grating (*i.e.*, the transmitted wavelength) is controlled from the PC (which masters the step motor of the monochromator) via a RS-232 interface. The optical signal that has passed through the monochromator is received by a broad bandwidth p-i-n photodiode connected to a preamplifier. Both elements are located in a removable head and are selected according to the wavelength range. The received signal via a band pass filter goes to the synchronous detector. The second input of the detector is from the reference channel mentioned at the beginning. The detector output is transferred through a low-pass filter to an A/D converter. In this way, the A/D converter output is proportional to the power of the received signal. The data obtained are transmitted via the microprocessor and RS 232 interface to the PC where they are used to display the spectrum of the measured element. This spectrum is corrected according to the photodetector responsivity versus wavelength characteristic.

The software that controls both the computer and monochromator works under Win95/Win98/WinNT4.0/Win2000. It makes it possible to process and display the spectra obtained. The software is written in object language Delphi with ×86 assembler procedures importer. The Open GL technique is used for fast display of 3D graphics. Therefore, the resulting code is less than 400 kB and the software runs correctly even on 486 PC with 100 MHz clock and 32 MB RAM. To fully use 3D graphics properties a hardware graphics accelerator is necessary that is compatible with Open GL. A part of the software resides in the Intel MCS51 microprocessor which belongs to the chopper and is used for the step motor control. The software operation is illustrated in Fig. 2, where a main loop is depicted. The user interface
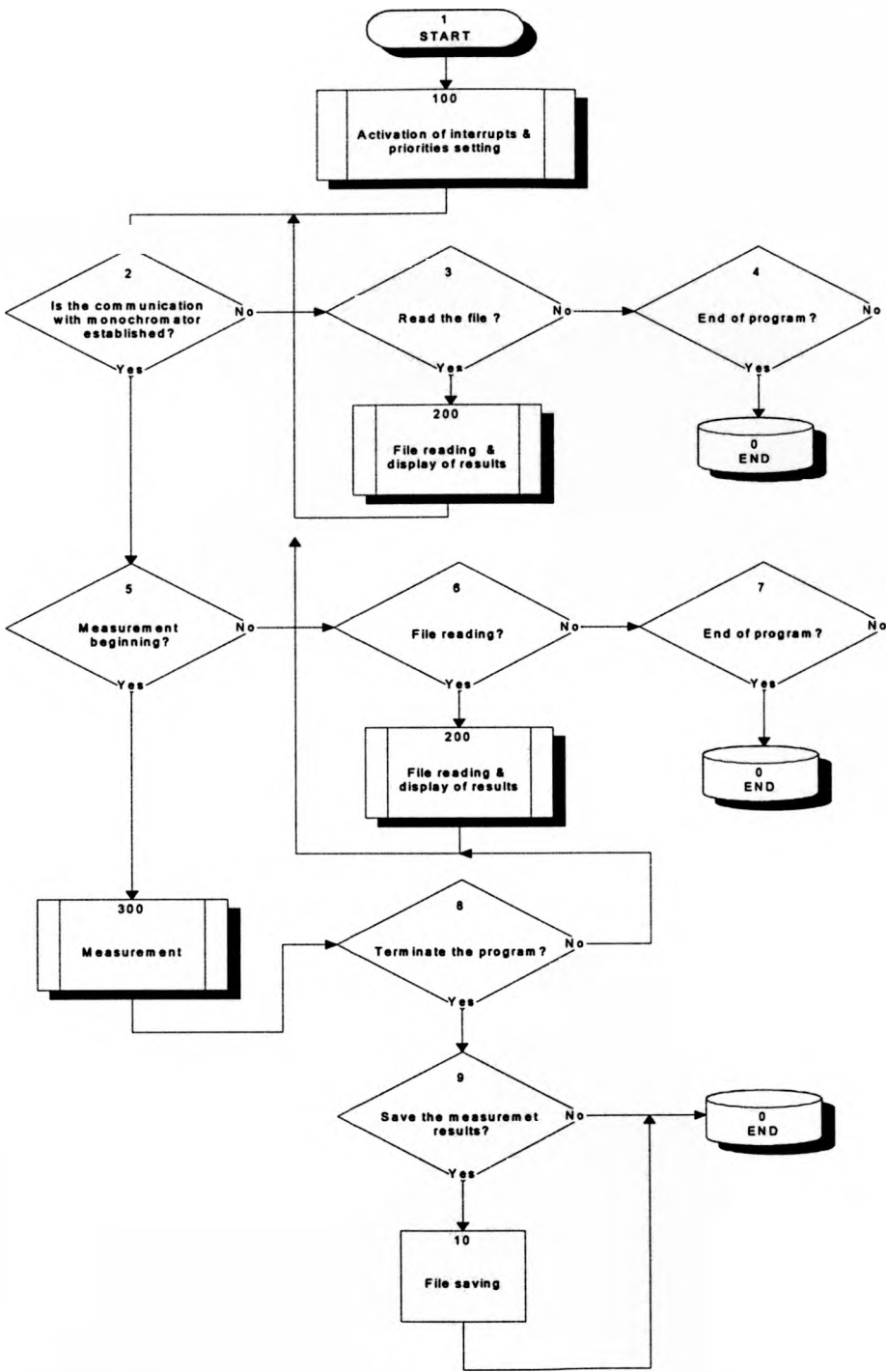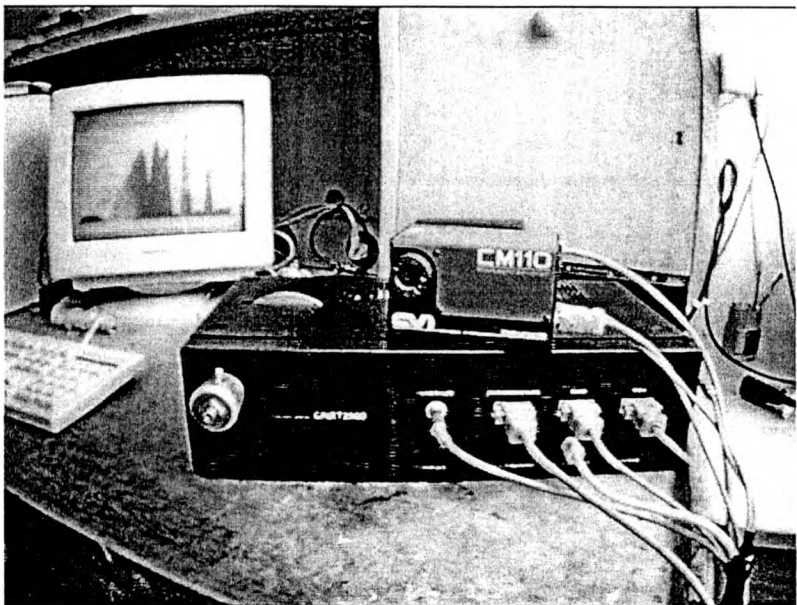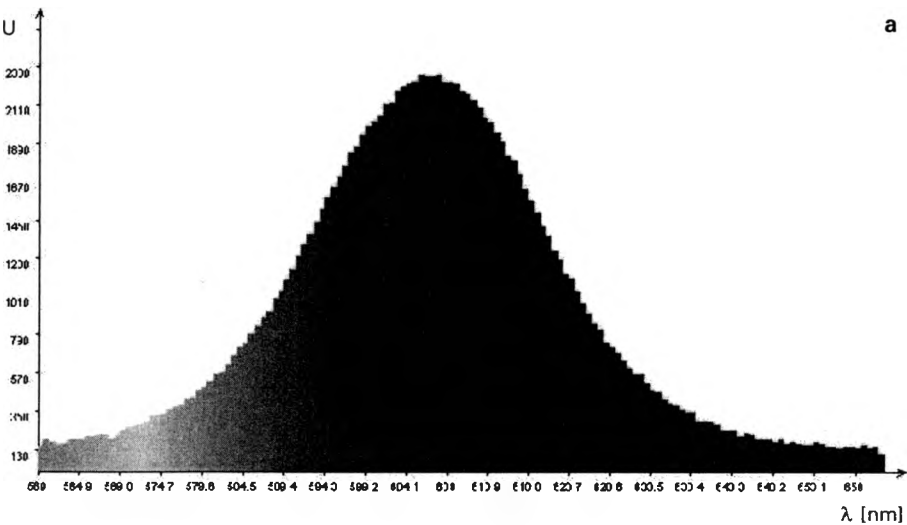
Fig. 2. Main loop of the software.

Fig. 3. Photograph of the instrument.

conforms to modern standards. The photo of the chopper itself is shown in Fig. 3. Examples of various light sources spectra measured by the instrument are depicted in Fig. 4a,b.
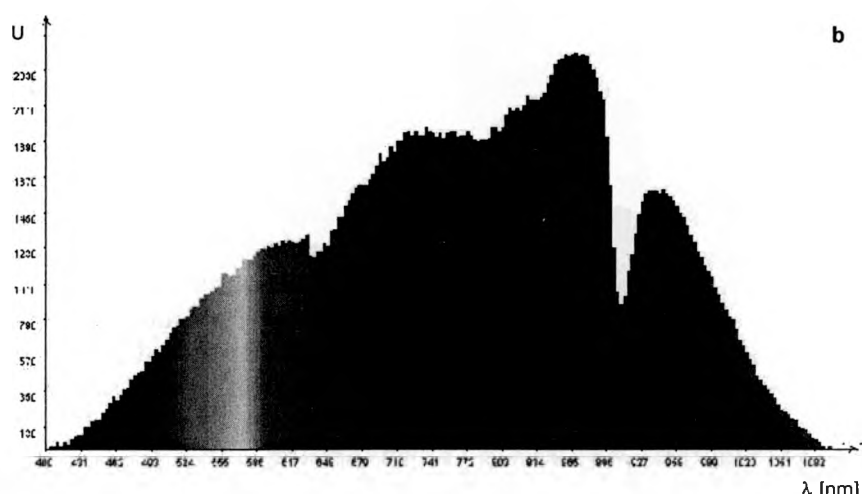

Fig. 4a

Fig. 4. Examples of measurement results: **a** — visible LED spectrum, **b** — spectrum of white light transmitted through a length of polymer fiber.

3. Design problems

3.1. Photoreceiver configuration selection

Here, two configurations are possible: high impedance (resistance) receiver and transimpedance receiver [2], [3]. The choice of configuration is forced by the photodetector parameters. For infrared an InGaAs photodiode, and for visible light a Si p-i-n photodiode were used. Due to the large photodiode area (3 mm in diameter) its capacitance was also large (up to 1 nF) and it turned out that the high impedance receiver had insufficient bandwidth. Therefore the transimpedance receiver was selected for realisation. The bandwidth of this receiver is determined by the Miller effect and is given by [2], [3]

$$B = \frac{k+1}{2\pi r C} \tag{1}$$

where k is the voltage gain of the amplifier. Thus, the bandwidth B is $\simeq k$ times greater than for a corresponding high impedance receiver.

3.2. Selection of the operating frequency

The noises of the photodetector and preamplifier are crucial factors. In general, the noise spectrum $N(f)$ may be approximated for low frequencies as [4]

$$N(f) = a\left(1 + \frac{f_d}{f}\right) \tag{2}$$

were a is a constant, and f_d is a cut-off frequency. From the data of various elements it follows that [4], [5] f_d is of the order of 100 ... 1000 Hz. It is obvious that the

operating frequency should be (much) greater than f_d. However, it cannot be very high as the noise factor F of the preamplifier increases with frequency due to the shunt capacitance C. Neglecting the low frequency noises, the noise factor of the preamplifier is given by [6]

$$F = \frac{i_d^2 + i_r^2 + i_n^2 + e_n^2(1/R_d^2 + 4\pi^2 f^2 C^2)}{i_d^2} \tag{3}$$

Here, $i_r^2 = 4kT/r$ (k — the Boltzman constant, T — temperature) is the thermal noise current of the feedback resistor r (transimpedance configuration) or load resistor r (high impedance configuration), e_n, i_n are the noise voltage and current of the preamplifier, $i_d = 2qI_c + 4kT/R_d$ is the photodiode noise current consisting of shot noise and thermal noise of its shunt resistance R_d (I_c is the dark current). In effect the operating frequency was selected around 300 Hz.

3.3. Preamplifier technology selection

It is obvious that the noise factor should be as low as possible. The values of e_n, i_n depend mainly on the technology used. For bipolar transistors e_n is a few nV/Hz$^{1/2}$, and i_n — a few pA/Hz$^{1/2}$; whereas for FET e_n is several nV/Hz$^{1/2}$, and i_n is 0.1... 10 fA/Hz$^{1/2}$ [5].

It follows from Equation (3) that the increase of the operating freqency (in this case above 1 kHz) is followed by the rise of noise factor F due to the shunt capacitance C. If the frequency f is below 1 kHz the noise current i_n is dominant because of the large value of R_d. Therefore, FET technology should be used as its value of i_n is orders of magnitude less than for bipolar. Additional FET advantages are high input resistance and low cut-off frequency f_d of the $1/f$ noise, especially for noise current.

3.4. Receiver dynamics

Another important factor that should be considered is a maximum signal level that may be received without distortions. The greater the transimpedance r the smaller this level is. The conclusion is simple: the photoreceiver that is noise optimised is not suitable for the detection of strong optical signals because of the possibility of overload. Therefore, we decided to employ removable heads with receivers that are interchangeable depending on the source wavelength and optical power.

3.5. Aperture shape

As the light flux from the examined source is modulated the question arises: what is the aperture shape that maximizes the fundamental harmonic power of the modulated signal $f(t)$? The maximum signal power is determined by the light source and monochromator properties. Therefore, it is necessary to find the maximum of the fundamental harmonic with the constraint of the maximum signal power P_{max} (α is the angle), i.e.

$$\int_0^\pi f(\alpha) \sin \alpha d\alpha = \max, \quad 0 < f(t) < P_{max}. \tag{4}$$

It is easy to show that the solution of this problem is given by a symmetrical rectangular signal with duty factor of 1/2. The power of such a signal at the electrical receiver is 2.1 dB greater than the power of the corresponding sine signal. In order to obtain such a signal it is necessary to eliminate transients between full opening and full closing of the rotating diaphragm. It follows that the diameter of the modulated beam should be possibly small as compared with the chopper openings.

4. Measurement errors

4.1. Monochromator errors

The precision of the wavelength measurement depends in the first place on the monochromator employed. Here, the Digikrom CM110 monochromator was used [1]. The manufacturer specifies the wavelength error as $+/-0.2$ nm. The resolution of the instrument is similar.

4.2. Precision of the spectral density measurement

To determine errors related to the measurement of the spectral density it is necessary to reconsider the principle of homodyne detection. As shown in Fig. 1, the input signal is multiplied by the reference in the mixer. The multiplication product is passed through a low pass filter in order to eliminate noise and higher harmonics. The random measurement error is a function of the noise spectral power density N', filter bandwidth B, and measured signal amplitude A, and is given by [7]

$$\sigma = \frac{\sqrt{BN'}}{A}. \tag{5}$$

The systematic error depends on the phase difference between the measured signal and the reference $\Delta\varphi$. In practice, the phase difference is small, and the relative systematic error δA_w may be approximated as (E is the statistical mean operator)

$$\delta A_w = \frac{E\{A\cos\Delta\varphi\} - A}{A} = \frac{E\{\cos(\Delta\varphi)\} - 1}{2} \approx \frac{E\{(\Delta\varphi)^2\}}{2} = \frac{\delta^2}{2}. \tag{6}$$

Here δ is the standard deviation of the phase difference $\Delta\varphi$ in radians. It follows that the systematic error depends on the variance of the phase difference fluctuation between signal and reference. Sometimes, the reference is obtained in a phase locked loop. This may lead to serious errors if the phase difference fluctuation is too large. Our instrument is immune to this problem as the reference is obtained by the modulation with the same chopper which is used to modulate the measured signal. If the chopper holes used for the signal and reference modulation have similar shapes and occupy the same angular positions, the measurement is not sensitive to the rotation velocity fluctuation. This is obvious since both groups are in the
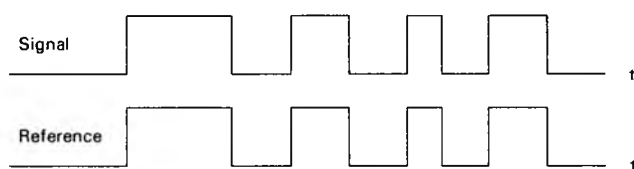
Fig. 5. Signal and reference changes due to the rotation velocity fluctuation.

same positions, and any phase change of the signal is followed by the same change of the reference phase, as is shown in Fig. 5. In practice, there are some mechanical tolerances of the dimensions of holes and positions on the rotating disc. However, they proved to be unimportant in this case.

4.3. Errors related to the photodiode responsivity

The readings of the instrument were corrected according to the function $R(\lambda)$, *i.e.*, the function of the photodiode responsivity versus the wavelength. However, if there are errors in $R(\lambda)$ due to aging, for example, they may lead to wavelength errors. In order to determine these errors let us assume that the spectral density $S(\lambda)$ near maximum λ_0 may be given by

$$S(\lambda) = 1 - \alpha(\lambda - \lambda_0)^2 \tag{7}$$

and the responsivity error ΔR may be approximated as

$$\Delta R = 1 + \beta(\lambda - \lambda_0). \tag{8}$$

Here, β stands for the slope error, and higher terms are neglected for simplicity. The resulting characteristic, as seen by the instrument, is

$$S_w(\lambda) = \Delta R \cdot S(\lambda) = [1 - \beta(\lambda - \lambda_0)][1 - \alpha(\lambda - \lambda_0^2)]. \tag{9}$$

The measurement error $\Delta\lambda$ of the center wavelength is the difference between maximum of the function (9) and the exact value of the central wavelength λ_0. Taking into account that α is related to the linewidth B (FWHM – full width at half maximum) via $\alpha = 2/B^2$ one can readily calculate the measurement error

$$\Delta\lambda = \frac{\beta}{2\alpha} = \beta\frac{B^2}{4}. \tag{10}$$

For example, if β equals 0.04/100 nm, the errors are as follows: for a multimode laser of $B = 5$ nm the error is 0.01 nm, and for a LED with linewidth of $B = 50$ nm the error is 1 nm. In the same manner we can calculate the linewidth measurement error. The calculus results (not included) show that this error is much smaller. It follows that the photodetector responsivity errors slightly move the spectrum along the wavelength axis but their influence on the spectrum linewidth is much smaller.

5. Conclusions

We have presented the chopper developed at the Telecommunications Institute of the Warsaw University of Technology. The instrument uses homodyne detection and due to unique design is insensitive to the phase difference fluctuation between the signal and the reference. Design problems have been discussed, including the selection of operating frequency, the optimisation of noise, and the choice of diaphragm shape. The error analysis showed that apart from the monochromator errors the most important are errors related to inaccurate photodiode responsivity function.

References

[1] CVI Laser Corporation, CM110 1/8 meter monochromator, handbook.
[2] MACLEAN D.J.H., *Optical Line Systems*, Wiley, Chichester 1996.
[3] LI T. [Ed.], *Topics in Lightwave Transmission Systems*, Academic Press, Bostaon 1991.
[4] MOTCHENBACHER C.D., FICHEN F.C., *Low-Noise Electronic Design*, Wiley, New York 1973.
[5] Texas Instruments & Maxim, Linear Circuit Data Book, catalogues.
[6] MOUSTAKES S., HULLET J.L., STEPHENS T.D., *Opt. Quant. Electron.* **14** (1982), 57.
[7] LINDSEY W.C., *Synchronization Systems in Communication and Control*, Prentice Hall, Englewood Ciffs, 1972.